

Direct evidence for critical exchange coupling via Al layers in the heavy-fermion compound CePd_2Al_3

S.A.M. Mentink, G.J. Nieuwenhuys, A.A. Menovsky,* and J.A. Mydosh
Kamerlingh Onnes Laboratory, Leiden University, P.O. Box 9506, 2300 RA Leiden, The Netherlands

H. Tou and Y. Kitaoka
Department of Material Physics, Faculty of Engineering Science, Osaka University, Toyonaka, Osaka 560, Japan
(Received 30 November 1993)

The long-range planar-type antiferromagnetic ordering in the heavy-fermion compound CePd_2Al_3 is shown to critically depend on the exact occupation and distribution of aluminum atoms over their available lattice sites. A polycrystalline sample ($T_N = 2.7$ K) is systematically compared with a nonordering single crystal, by means of susceptibility, specific heat and site-specific Al-NQR/NMR experiments. Implications for other Al-containing heavy-fermion systems are discussed.

I. INTRODUCTION

The hexagonal intermetallic compound CePd_2Al_3 is characterized as a heavy-electron antiferromagnet^{1,2} with $\gamma \simeq 340$ mJ/molK,² and belongs to the same family as the magnetic superconductor UPd_2Al_3 .³ The PrNi_2Al_3 -type crystal structure consists of cerium-palladium layers, alternating along the c direction with isolated aluminum layers. Antiferromagnetic (AF) ordering below $T_N = 2.7$ K of cerium moments ($\approx 0.5\mu_B$) was found in annealed polycrystals, whereas single crystals remain paramagnetic down to 0.4 K.^{4,5} The other relevant energy scales, as could be estimated from bulk experiments, are the Kondo temperature $T_K = 19$ K and crystal-field splitting energy $\Delta_1 = 33$ K and $\Delta_2 \gtrsim 600$ K. Here we report on the origin of the striking differences between polycrystal- and single-crystal samples of CePd_2Al_3 .⁶ While metallurgical analysis and neutron diffraction only hint at the role of Al, it is the splitting of the ²⁷Al nuclear quadrupole resonance (NQR) frequency in zero field that demonstrates a subtle distinction in Al-site occupation between the polycrystal- and single-crystal samples.

The magnetism of CePd_2Al_3 belongs to the planar class with weak interplane magnetic exchange coupling, J_z . We therefore ascribe the criticality of J_z to a different occupation and distribution of Al atoms over two possible sites. The same effect is proposed for the different superconducting transition temperatures T_c in various UPd_2Al_3 samples.⁷ The ferromagnetic (FM) character of CePd_2Ga_3 (Ref. 8) and pressure experiments on CePd_2Al_3 (Ref. 9) are taken as further evidence for our model.

II. CRYSTALLOGRAPHIC AND MAGNETIC STRUCTURE

Polycrystalline (PC) samples of CePd_2Al_3 were prepared by arc melting the pure (Ce:4N, Pd:5N, Al:6N)

elements, with initial stoichiometry 1:2:3, one of which (PC1) was annealed at 800 °C for 1 week. Two single crystals, SC1 and SC2, were grown with the tri-arc Czochralski method, using 2% excess of aluminum in the starting material to compensate for Al evaporation. No effect of heat treatment was observed in any of the experimental properties of single crystals. Annealed SC1 was used for bulk experiments and neutron diffraction, while SC2 was studied by NMR and $\mu^+\text{SR}$.¹⁰ Table I lists the various samples with analyzed composition and lattice parameters. Single crystals are homogeneous and contain approximately 3 at. % less aluminum than polycrystals.

Structure refinement of powder neutron diffraction, performed on annealed polycrystalline samples from different sources, have been published by Dönni *et al.*¹¹ The neutron diffraction results were indexed with the ideal PrNi_2Al_3 -type crystal structure and correct 1:2:3 stoichiometry, and are in good agreement with the x-ray data. Note that the absolute compositions of Table I determined by electron probe microanalysis (EPMA) slightly differ from 1:2:3, probably due to complicated corrections inherent to this method. We therefore stress that only the *relative* compositions among the various samples of Table I should be considered as significant. The AF structure below $T_N = 2.8(1)$ K, determined by Mitsuda *et al.*¹² and Dönni *et al.*,¹¹ resembles that of

TABLE I. Electron probe microanalysis, heat treatment, and lattice parameters indexed by the PrNi_2Al_3 structure (x-ray diffraction) of various samples of CePd_2Al_3 and annealed polycrystalline LaPd_2Al_3 .

Sample	Composition	Heat treatment	a (Å)	c (Å)
PC1	$\text{Ce}_{0.98}\text{Pd}_{1.92}\text{Al}_{3.10}$	800 °C/1 week	5.470	4.216
PC2	$\text{Ce}_{0.98}\text{Pd}_{1.94}\text{Al}_{3.09}$	as-cast	5.477	4.222
SC1	$\text{Ce}_{1.03}\text{Pd}_{2.00}\text{Al}_{2.97}$	1000 °C/1 week	5.473	4.216
SC2	$\text{Ce}_{1.06}\text{Pd}_{1.99}\text{Al}_{2.96}$	as-grown	5.469	4.214
PC3	$\text{La}_{0.99}\text{Pd}_{1.92}\text{Al}_{3.09}$	800 °C/1 week	5.500	4.224

UPd₂Al₃.¹³ The cerium moments align in the basal plane, with ordering k vector $(0,0,\frac{1}{2})$. The FM planes are coupled antiferromagnetically along the c axis. The ordered cerium moment, μ_{ord} , at 1.5 K is $0.47 \mu_B$,¹¹ reflecting a rather strong Kondo effect. No evidence for an incommensurate magnetic structure was found (see Ref. 13 for UPd₂Al₃). Neutron-diffraction experiments on SC1 showed a large reduction of the strongest (002) reflection.⁴ This partially results from extinction, but it also indicates that aluminum atoms are statically or dynamically displaced from the $z = 1/2$ plane. Long-range magnetic order was not detected down to 1.5 K, by neutron scattering on SC1 (Ref. 4) or from zero-field μ^+ SR on SC2.¹⁰

III. RESULTS

The susceptibility, $\chi \equiv M/H$, was measured on PC1 and SC1 along the a and c axes of the hexagonal lattice, in an external field of 0.5 T. Figure 1 displays the various $\chi(T)$ up to 25 K. The strong anisotropy of the magnetic moment is reflected in the large response along the a axis compared to the c axis. For PC1, a downward kink signals long-range AF order below $T_N = 2.7$ K. Above 100 K (not shown) χ is proportional to $1/T$, with effective moment $2.37 \mu_B/\text{f.u.}$ and Curie-Weiss temperature -30.3 K. As the reference compound LaPd₂Al₃ is Pauli paramagnetic with small $\chi_P = 2.3 \times 10^{-9} \text{ m}^3/\text{mol}$, this moment can be fully assigned to cerium. Figure 1 shows the ever-increasing paramagnetic behavior of SC1 down to 1.6 K. As-cast PC2 behaves similarly.² χ can be satisfactorily described by a crystal-field-split ground state $\Gamma_7 = |\pm 1/2\rangle$ and excited states $\Gamma_9 = |\pm 3/2\rangle$ at 33 K and $\Gamma_8 = |\pm 5/2\rangle$ at 800 K. Inelastic neutron scattering confirmed the lower excitation energy and placed a lower limit of ≈ 600 K on the overall splitting.¹⁰

CePd₂Al₃ is classified as a heavy-fermion antiferromagnet^{1,2} by its large electronic specific heat coefficient $\gamma \simeq 340 \text{ mJ/molK}^2$. Figure 2 depicts c/T versus temperature below 10 K for both PC1 and SC1. Note the sharp peak at T_N for PC1 and the increasing c/T for SC1. The estimated entropy released in the magnetic transition, $S_{\text{ord}} = 0.35R \ln 2$ (indicating reduced-moment ordering), is smeared out in single crystals. Here c/T

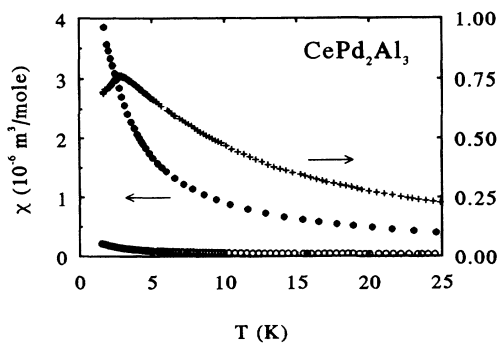


FIG. 1. Susceptibility of polycrystal PC1 (+) and single-crystal (SC1) CePd₂Al₃ along the main crystallographic directions a (•) and c (◊).

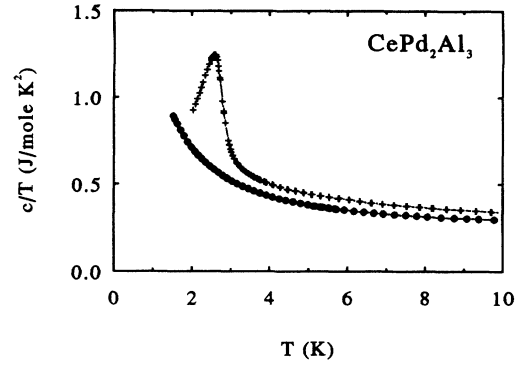


FIG. 2. Specific heat divided by temperature versus temperature for polycrystal PC1 (+) and single-crystal SC1 (•) CePd₂Al₃.

reaches 900 mJ/mol K^2 at 1.5 K. The proximity to a magnetic transition suggests that the entropy involved is mainly of magnetic origin, stemming from in-plane magnetic fluctuations, in accordance with the slowly increasing zero-field μ^+ -relaxation rate.¹⁰

Its site-specific nature makes NMR and NQR the ideal techniques to probe the influence of the isolated aluminum layer on the magnetic and superconducting properties of 1:2:3 materials.^{14,15} A $1/T_1$ study on polycrystalline CePd₂Al₃ was performed in Ref. 16, where a Kondo temperature $T_K = 20$ K was estimated. The NMR spectra on fine powders of PC1, PC2, and SC2 were obtained by tracing the spin-echo intensity as a function of magnetic field at a fixed frequency, while the NQR spectra result from the spin-echo signal as a function of frequency in zero field. Due to the electric quadrupole moment of ²⁷Al, any inhomogeneous internal electric-field gradient in the lattice will affect the NQR lines. A single line from the transition of m_I states $|\pm 3/2\rangle \leftrightarrow |\pm 5/2\rangle$, will (i) *split* if there is more than one unique field gradient (this may be interpreted as the occurrence of more than one Al site with different point symmetries) and (ii) *broaden* if the electric-field gradient is inhomogeneous.

Both effects combine into split, broadened lines when multiple positions are inequivalently occupied and the surrounding charges are inhomogeneously distributed. Figure 3, which displays a systematic variation of the NQR spectra for PC1, PC2, and SC2, shows precisely this effect. All spectra are composed of two peaks at 2.01 and 1.91 MHz. However, the linewidth and relative intensity of the lower satellite peak significantly increase as summarized in Table II. Surprisingly and in contrast with the structure refinements, the split transition in the NQR spectrum proves that the aluminum atoms experience two inequivalent electric-field gradients, most likely associated with the Al-site occupation. A similar but smaller effect is found in UT₂Al₃ ($T = \text{Ni, Pd}$) compounds.¹⁵ As neutron diffraction rules out any structural symmetry lowering or atomic-site interchange, within the inherent detection limit, a more subtle deviation from the ideal PrNi₂Al₃ structure must be in-

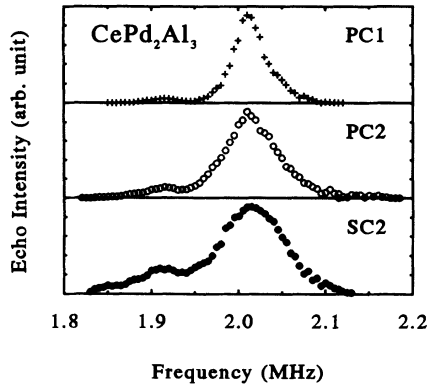


FIG. 3. NQR spectra for the $|\pm 3/2\rangle \leftrightarrow |\pm 5/2\rangle$ transition of ^{27}Al in powdered CePd_2Al_3 samples. (+) denotes annealed PC1 and (o) as-cast PC2. Single-crystal SC2 is depicted by (•). Note the presence of two lines, with different widths for all samples.

ferred. We propose that the Al atoms can rearrange over two sites, induced by either disorder (PC2) or vacancies (SC2). The lattice symmetry remains unchanged if the Al atoms slightly displace in the c direction, previously indicated from the single-crystal neutron diffraction.⁴ Then the satellite peak in the NQR frequency is due to the change of the electric-field gradient at the Al nucleus caused by the surrounding Al atoms and/or the mixing effect with Ce- $4f$ states.

Our NMR data in the field (not shown) on PC1 agree with Ref. 16. However, as-cast PC2, which does not undergo a long-range AF transition, exhibits a large distribution of spin-lattice relaxation times T_1 below the same $T_N = 2.7$ K. This reflects the presence of short-range magnetic correlations and the proximity of the AF ordering.^{2,6}

IV. DISCUSSION

In order to construct a suitable model for the magnetism of CePd_2Al_3 , we use the following ingredients.

(i) The cerium atoms form a regular hexagonal lattice, with the magnetic moments directed parallel to the hexagonal plane.

(ii) The palladium atoms are very close to cerium (much closer than in, e.g., the CeT_2X_2 series¹⁷), implying strong in-plane f - d hybridization, J_{f-d} .

TABLE II. NQR linewidth (main peak) and relative intensities of the main and satellite peaks for annealed (PC1) and quenched (PC2) polycrystals, and single-crystal (SC2) CePd_2Al_3 .

Sample	Linewidth (kHz)	Relative intensity (%)	
		Main	Satellite
PC1	40	93.5	6.5
PC2	65.7	88.8	11.2
SC2	85.7	76.5	23.5

(iii) The aluminum atoms are situated close to the $z = 1/2$ plane, isolated from the other atoms.

(iv) The aluminum atoms can occupy two sites, depending on the degree of disorder and the amount of Al vacancies.

The magnetic ordering temperature in the Doniach model for a one-dimensional array of Kondo ions is governed by the competing Kondo and Ruderman-Kittel-Kasuya-Yosida (RKKY) interactions, leading to the “Kondo-necklace” phase diagram.¹⁸ We earlier determined that CePd_2Al_3 , if placed in this phase diagram, should be situated on the right-hand side of the maximum ordering temperature, close to the magnetic-nonmagnetic phase boundary,¹⁰ due to the large in-plane hybridization J_{f-d} . The large J_{f-d} is used here *only* to explain the reduced ordered moment and rather large Kondo temperature. The reduced cerium moments are confined to the basal plane and are magnetically correlated in these planes at low temperatures. However, long-range three-dimensional magnetic order can only be generated by the magnetic exchange parameter J_z , which couples the magnetic planes via the aluminum layer. This coupling involves RKKY-type interactions between the partially hybridized magnetic f electron of cerium with the s, p -electron cloud of the aluminum atoms.

The Doniach phase diagram is a one-dimensional model, in which anisotropic exchange is not incorporated. Therefore, our results cannot be understood by the Doniach model alone. We propose that the large anisotropy of CePd_2Al_3 , to a first approximation, allows for a separate treatment of the two interactions: the f - d electron-band hybridization J_{f-d} in the basal plane, and the magnetic exchange, J_z , between the planes. This analysis is similar to the existence of two nearly separate subsystems of (hybridized) $5f$ -quasiparticle states in homologous UPd_2Al_3 , proposed to cause the increase of both T_N and γ with increasing hydrostatic pressure.¹⁹ Obviously, in a more sophisticated description of Kondo lattices, the effects of the different anisotropic exchange interactions should be connected. To the best of our knowledge such a theory has not yet been developed. In the favorable cases of CePd_2Al_3 and UPd_2Al_3 with their large crystallographic and magnetic anisotropy, the conjecture of two nearly independent exchange parameters is believed to be justified.

The extreme sample dependence of AF ordering and the small value of $T_N = 2.7$ K of CePd_2Al_3 indicate that J_z is small, as opposed to the large J_{f-d} . As the magnetic correlations build up because of the polarization of the (mainly) aluminum s, p -like conduction-electron cloud between two magnetic layers, any irregularity in that layer will obstruct magnetic ordering.

The differences in magnetic behavior between the various samples in Tables I and II can now be explained.

(i) In annealed polycrystals (PC1) a stoichiometric amount of Al is *almost fully* distributed over the $3(g)$ site in the PrNi_2Al_3 structure. This produces a well-defined electronic environment in which long-range anti-ferromagnetism can develop. The magnetic correlation length along the c axis, ξ_c , is infinite.

(ii) In as-cast polycrystals (PC2) there are clearly two

Al sites (Fig. 3) with *random* occupation. This leads to an irregular electronic environment, thereby reducing the average coupling strength between the planes, $\langle J_z \rangle$. Here magnetic correlations exist, but long-range order is prevented and ξ_c remains finite.^{2,6}

(iii) In annealed (SC1) or as-grown (SC2) single crystals it is the Al *deficiency* which generates two Al sites with highly inhomogeneous local electronic environment. This diminishes the interplanar coupling strength $\langle J_z \rangle$ below its critical value; thus $\xi_c \rightarrow 0$.

The above model is consistent with two independent experiments. First, if an atom with both a larger spatial extension and density of conduction-electron states (e.g., Ga) is substituted for Al, the coupling strength should increase.²⁰ The observed FM ground state of CePd₂Ga₃ below $T_C = 6$ K (Ref. 8) indicates a twice stronger J_z . Note that the crystalline electric field (CEF) splitting and moment direction are similar to that of CePd₂Al₃.

Second, the application of hydrostatic pressure influences both magnetic coupling and the hybridization. If the pressure dependences of J_z and J_{f-d} have opposite sign, an anomalous pressure dependence of T_N may result. An increase of pressure leads to an increase of the hybridization J_{f-d} . The pressure dependence of J_z may have positive or negative sign, depending on the details of the damped oscillatory RKKY interaction. The influence of hydrostatic pressure on both resistivity and specific heat has been investigated on annealed samples from different sources.^{9,21} A moderate pressure of 5.4 kbar enhances T_N of PC1 from 2.7 K to 2.8 K (with rate +0.02 K/kbar), without affecting the magnetic entropy, S_{ord} . Above 8 kbar, T_N starts to decrease by

−0.1 K/kbar, and S_{ord} falls rapidly to zero. This non-monotonic behavior of T_N suggests the presence of two competing effects, which can be readily explained by our model with near-independent anisotropic exchange. It suggests a large positive pressure dependence of J_z , causing the initial increase of T_N . The subsequent decrease of T_N is proposed to result from an increasing J_{f-d} , which reduces both μ_{ord} and S_{ord} .

In conclusion, we have demonstrated the close relationship between subtle structural effects and magnetic ordering in CePd₂Al₃ by macroscopic and microscopic experimental methods. The presented model incorporates a second magnetic exchange parameter J_z , in addition to the *f-d* electron-band hybridization J_{f-d} . Our model is thought to be valid in the limit of strong crystallographic and magnetic anisotropy. It is suggested to be applicable to all 1:2:3 materials with nearly local moments, viz., CePd₂Al₃, CePd₂Ga₃, and UPd₂Al₃, where the superconducting transition temperature strongly depends on Al concentration.^{7,10} A similar situation exists in CeAl₃ where single crystals having one Al-NMR signal show AF order,²² while polycrystals with more than one NQR component do not.²³

ACKNOWLEDGMENTS

This work was partially supported by the Dutch Foundations FOM and NWO. We acknowledge P. Fischer and P. Böni for valuable discussions and C. Wassilew for making available the unpublished pressure data.

* Also at Van der Waals–Zeeman Laboratory, University of Amsterdam, Valckenierstraat 65, 1018 XE Amsterdam, The Netherlands.

¹ H. Kitazawa, C. Schank, S. Thies, B. Seidel, C. Geibel, and F. Steglich, *J. Phys. Soc. Jpn.* **61**, 1461 (1992).

² S.A.M. Mentink, N.M. Bos, G.J. Nieuwenhuys, A.A. Menovsky, and J.A. Mydosh, *Physica B* **186-188**, 497 (1993).

³ C. Geibel, C. Schank, S. Thies, H. Kitazawa, C.D. Bredl, A. Böhm, M. Rau, A. Grauel, R. Caspary, R. Helfrich, U. Ahlheim, G. Weber, and F. Steglich, *Z. Phys. B* **84**, 1 (1991).

⁴ S.A.M. Mentink, N.M. Bos, G.J. Nieuwenhuys, A. Drost, F. Frikkee, L.T. Tai, A.A. Menovsky, and J.A. Mydosh, *Physica B* **186-188**, 460 (1993).

⁵ H. Kitazawa, A. Mori, S. Takano, T. Yamadaya, A. Matsushita, T. Matsumoto, N. Sato, T. Komatsubara, C. Schank, C. Geibel, and F. Steglich, *Physica B* **186-188**, 612 (1993).

⁶ S.A.M. Mentink *et al.* (unpublished).

⁷ T. Sakon, K. Imamura, N. Takeda, N. Sato, and T. Komatsubara, *Physica B* **186-188**, 297 (1993).

⁸ E. Bauer, R. Hauser, E. Gratz, G. Schaudy, M. Rotter, A. Lindbaum, D. Gignoux, and D. Schmitt, *Z. Phys. B* **92**, 411 (1993).

⁹ F. Nolting, A. Eichler, S.A.M. Mentink, and J.A. Mydosh, *Physica B* (to be published).

¹⁰ S.A.M. Mentink, G.J. Nieuwenhuys, A.A. Menovsky, J.A. Mydosh, A. Drost, E. Frikkee, Y. Bando, T. Takabatake, P. Böni, P. Fischer, A. Furrer, A. Amato, and A. Schenk, *Physica B* (to be published).

¹¹ A. Dönni, P. Fischer, B. Roessli, and H. Kitazawa, *Z. Phys. B* **93**, 449 (1994).

¹² S. Mitsuda, T. Wada, K. Hosoya, H. Yoshizawa, and H. Kitazawa, *J. Phys. Soc. Jpn.* **61**, 4667 (1992).

¹³ A. Krimmel, P. Fischer, B. Roessli, H. Maletta, C. Geibel, C. Schank, A. Grauel, A. Loidl, and F. Steglich, *Z. Phys. B* **86**, 161 (1992); A. Krimmel, A. Loidl, P. Fischer, B. Roessli, A. Dönni, H. Kita, N. Sato, Y. Endoh, T. Komatsubara, C. Geibel, and F. Steglich, *Solid State Commun.* **87**, 829 (1993).

¹⁴ Y. Kitaoka, K. Ueda, T. Kohara, Y. Kohori, and K. Asayama, in *Theoretical and Experimental Aspects of Valence Fluctuations and Heavy-fermions*, edited by L.C. Gupta and S.K. Malik (Plenum, New York, 1987), p. 297.

¹⁵ M. Kyogaku, Y. Kitaoka, K. Asayama, C. Geibel, C. Schank, and F. Steglich, *J. Phys. Soc. Jpn.* **62**, 4016 (1993).

¹⁶ K. Fujiwara, Y. Yamanashi, and K. Kumagai, *Physica B* (to be published).

¹⁷ T. Endstra, G.J. Nieuwenhuys, and J.A. Mydosh, *Phys. Rev. B* **48**, 9595 (1993).

¹⁸ S. Doniach, in *Valence Instabilities and Related Narrow-Band Phenomena*, edited by R.D. Parks (Plenum, New

- York, 1977) p. 169.
- ¹⁹ R. Caspary, P. Hellmann, M. Keller, G. Sparn, C. Wassilew, R. Köhler, C. Geibel, C. Schank, F. Steglich, and N.E. Phillips, *Phys. Rev. Lett.* **71**, 2146 (1993).
- ²⁰ Strong support for this idea is found in the increasing T_N with Ga concentration in $\text{CeAl}_{2-x}\text{Ga}_x$: M.A. Fremy, D. Gignoux, D. Schmitt, and A.Y. Takeuchi, *J. Magn. Magn. Mater.* **82**, 175 (1989), and references therein.
- ²¹ C. Wassilew (private communication).
- ²² G. Lapertot, R. Calemczuk, C. Marcenta, J.Y. Henry, J.X. Boucherle, J. Flouquet, J. Hammann, R. Cibir, J. Cors, D. Jaccard, and J. Sierro, *Physica B* **186-188**, 454 (1993).
- ²³ J. Hunziker, J.L. Gavilano, S. Büchi, and H.R. Ott, *Physica B* **194-196**, 273 (1994).